Quantification of ^{123}I-PE2I Binding to Dopamine Transporter with SPECT After Bolus and Bolus/Infusion

Lars H. Pinborg, MD[1]; Morten Ziebell, MD[1]; Vibe G. Frøkjær, MD[1]; Robin de Nijs, MS[1]; Claus Svarer, MS, PhD[1]; Steven Haugbøl, MD[1]; Stig Yndgaard, MD[2]; and Gitte M. Knudsen, MD, PhD[1]

[1]Neurobiology Research Unit, University Hospital Rigshospitalet, Copenhagen, Denmark; and [2]Department of Anesthesia, University Hospital Rigshospitalet, Copenhagen, Denmark

The aim of the present study was to describe a method combining easy implementation in a clinical setting with accuracy and precision in quantification of ^{123}I-labeled *N*-(3-iodoprop-(2E)-enyl)-2β-carboxymethoxy-3β-(4′-methylphenyl)nortropane (PE2I) binding to brain dopamine transporter. **Methods:** Five healthy subjects (mean age, 50 y; range, 40–68 y) were studied twice. In the first experiment, dynamic SPECT data and arterial plasma input curves obtained after ^{123}I-PE2I bolus injection were assessed using Logan, kinetic, transient equilibrium, and peak equilibrium analyses. Accurate and precise determination of BP_1 (binding potential times the free fraction in the metabolite-corrected plasma compartment) and BP_2 (binding potential times the free fraction in the intracerebral nonspecifically bound compartment) was achieved using Logan analysis and kinetic analysis, with a total study time of 90 min. In the second experiment, ^{123}I-PE2I was administrated as a combined bolus and constant infusion. The bolus was equivalent to 2.7 h of constant infusion. **Results:** The bolus-to-infusion ratio of 2.7 h was based on the average terminal clearance rate from plasma in the bolus experiments. Steady state was attained in brain and plasma within 2 h, and time–activity curves remained constant for another 2 h. Even when an average bolus-to-infusion ratio was used, the striatal BP_1 and BP_2 values calculated with kinetic analysis ($BP_1 = 21.1 \pm 1.1$; $BP_2 = 4.1 \pm 0.4$) did not significantly differ from those calculated with bolus/infusion analysis ($BP_1 = 21.0 \pm 1.2$; $BP_2 = 4.3 \pm 0.3$). Computer simulations confirmed that a 2-fold difference in terminal clearance rate from plasma translates into only a 10% difference in BP_1 and BP_2 calculated from 120 to 180 min after tracer administration. **Conclusion:** The bolus/infusion approach allows accurate and precise quantification of ^{123}I-PE2I binding to dopamine transporter and is easily implemented in a clinical setting.

Key Words: ^{123}I-PE2I; dopamine transporter; SPECT; kinetic analysis; Logan analysis; bolus/infusion analysis

J Nucl Med 2005; 46:1119–1127

The tropane analog *N*-(3-iodoprop-(2E)-enyl)-2β-carboxymethoxy-3β-(4′-methylphenyl)nortropane (PE2I) binds with high affinity to the neuronal dopamine transporter (DAT) (inhibition constant [K_i] = 17 nmol/L) and with much lower affinity to the serotonin transporter (29-fold) and the noradrenaline transporter (>58-fold) (*1*). In vivo, PET and SPECT studies on healthy subjects have demonstrated excellent kinetic properties for ^{11}C-PE2I (*2*) and ^{123}I-PE2I (*3–5*). Time–activity curves showed that striatum-specific binding peaked approximately 60 min after bolus injection and that, for PET, the striatum-to-cerebellum ratio was approximately 10 at peak time (*2*). The usefulness of the cerebellum and neocortex as reference regions has been demonstrated in monkeys, in which the striatal time–activity curves after ^{11}C-PE2I injection reached the level of the cerebellum and neocortex after injection of unlabeled 2β-carbomethoxy-3β-(4-iodophenyl)tropane (β-CIT). In addition, the cerebellar and neocortical time–activity curves were unchanged after injection of unlabeled β-CIT (*2*). This finding agrees with the very low ^{125}I-PE2I binding seen in the neocortex and cerebellum on human whole-hemisphere autoradiography (*6*). Only polar plasma metabolites of ^{11}C-PE2 (*2*) and ^{123}I-PE2I (*7*), unlikely to cross the blood–brain barrier to any significant extent, have been demonstrated. In baboons, in vivo striatal ^{11}C-PE2I B'_{max} values correlated with in vivo striatal 6-^{18}F-fluoro-L-dopa K_i values, with in vitro striatal ^{125}I-PE2I B_{max} values, and with the number of tyrosine hydroxylase–immunoreactive neurons in the substantia nigra (*8*). ^{123}I-PE2I has proven useful for preclinical and early diagnosis of Parkinson's disease in humans (*5*) and experimental Parkinson's disease in monkeys (*5,9*).

The aim of this study was to describe a method that provides a reliable quantitative estimate of receptor parameters and is easy to implement in a clinical setting. We present results from 5 healthy subjects who underwent SPECT twice: first after a bolus injection of ^{123}I-PE2I and then, days or weeks later, after a bolus injection plus a constant infusion of ^{123}I-PE2I. The ratio of the bolus size (MBq) to the infusion velocity (MBq/h) is defined as the

Received Dec. 14, 2004; revision accepted Mar. 29, 2005.

For correspondence or reprints contact: Lars H. Pinborg, MD, Neurobiology Research Unit, Rigshospitalet, N9201, 9 Blegdamsvej, Copenhagen, DK-2100 Denmark.

E-mail: pinborg@nru.dk

bolus-to-infusion ratio (h). The bolus-to-infusion ratio used in all bolus/infusion studies was determined from the average kinetic parameters of the initial bolus studies. The design of the study allowed direct comparison of binding potential (BP) after bolus and BP after bolus/infusion in each individual. The design also allowed comparison of use of the average bolus-to-infusion ratio and use of the theoretic optimal bolus-to-infusion ratio calculated from an individual's terminal clearance rate of ^{123}I-PE2I from plasma.

MATERIALS AND METHODS

Subjects

Five healthy subjects (mean age, 50 y; range, 40–68 y) were included in the study. All claimed to be alcohol and drug free, had no history of neurologic or psychiatric disorders, had normal results on physical examination and routine blood tests, and gave written informed consent. The study was performed in accordance with the ethical standards of the Declaration of Helsinki and was approved by the ethical committee of Copenhagen and Frederiksberg (KF 02-150/98).

Experimental Procedures

SPECT was performed using a triple-head IRIX SPECT scanner (Philips Medical Systems) fitted with general-purpose low-energy, parallel-hole collimators (spatial resolution, 8.5 mm at 10 cm). The imaging energy window was positioned at 143–175 keV. High-energy photons of ^{123}I penetrated through the lead of the collimator, and Compton scatter in the scintillation crystal caused erroneous counts in the imaging energy window. A second energy window positioned at 184–216 keV was used to correct for these high-energy photons in the imaging window. Projection data were recorded at 120 angles with an interval of 3°. Before reconstruction, the projection images of the 2 energy windows were subtracted. Reconstruction of the images was performed in MATLAB 6.5 (MathWorks) in 128 × 128 matrices (2.33-mm pixels and identical slice thickness) using standard filtered backprojection with a low-pass fourth-order Butterworth filter at 0.3 Nyquist (0.064/mm) and using uniform attenuation correction with an attenuation coefficient of 0.10/cm.

The system resolution at 10 cm from the collimator and 1 cm off center was 12 mm in full width at half maximum in the radial direction and 8 mm in full width at half maximum in the transverse and tangential directions. Figure 1 shows a representative SPECT image after bolus/infusion of ^{123}I-PE2I.

All subjects were studied twice, on 2 separate days. To block thyroidal uptake of free radioiodine, we gave 200 mg of potassium perchloride intravenously to all subjects 30 min before the ^{123}I-PE2I injection. In the first experiment, an average bolus of 138.3 MBq (range, 128.5–144.4 MBq) of ^{123}I-PE2I (MAP Medical Technologies) was administrated intravenously to all subjects. Tracer was delivered over a period of 10 s. Twenty-one sequential scan frames were acquired from 0 to 180 min after bolus injection. The frame durations were 6 × 5 min and 15 × 10 min. Great care was taken to ensure that each subject was aligned in the same position during the whole scan session by placing the subject's head within a support. A cannula was inserted into the radial artery for arterial blood sampling. Thirty-six arterial blood samples were collected from 0 to 180 min after bolus injection. During the first 2 min, 12 arterial blood samples were collected; from 2 to 35 min, 10 arterial blood samples were collected; and from 35 to 175 min, arterial blood samples were collected every 10 min. Octanol was extracted from the plasma to derive the lipophilic phase containing ^{123}I-PE2I (*7*). One milliliter of plasma and 2 mL of octanol were shaken for 2 min, and then 1 mL of the octanol phase was pipetted into another counting vial. The activity in the octanol phase, multiplied by 2, thus represented parent ^{123}I-PE2I. In the bolus-infusion experiments, conducted more than 3 wk later, an average bolus of 73.9 MBq (range, 63–93.8 MBq) of ^{123}I-PE2I was followed by a constant infusion of ^{123}I-PE2I for 3 h. The bolus-to-infusion ratio was 2.7 h (range, 2.6–2.8 h). In all experiments, the specific radioactivity was greater than 8.7 TBq/μmol. Eighteen sequential 10-min scan frames were collected from 60 to 240 min after tracer injection. Two cannulae were inserted into the cubital veins for tracer administration and venous blood sampling. Twenty-four venous blood samples were collected from 0 to 240 min after tracer injection. Metabolite correction was done. Plasma protein binding was not determined.

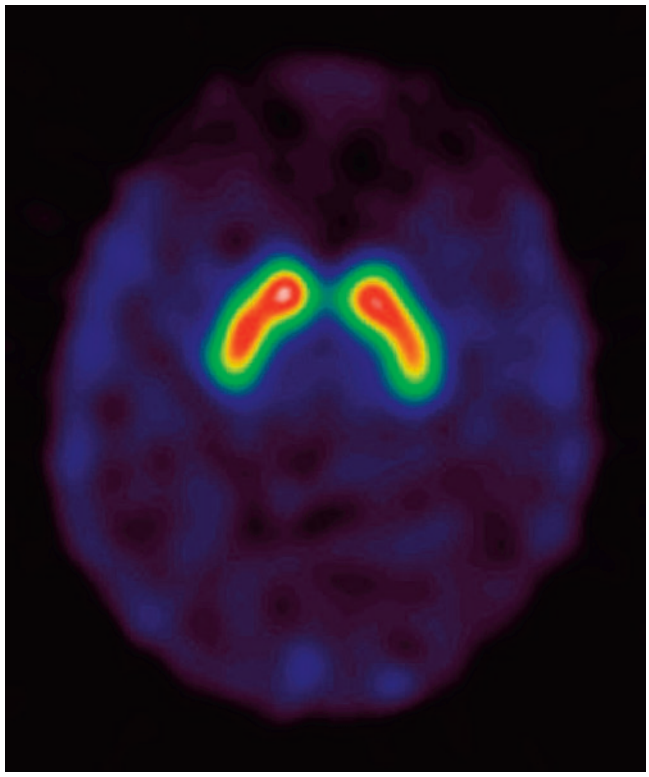

FIGURE 1. ^{123}I-PE2I SPECT image obtained from 2 to 3 h after tracer injection in healthy subject.

Regions of Interest (ROIs)

The individual bolus SPECT images and bolus/infusion SPECT images were manually aligned using software supplied with the scanner. Subsequently, the individual SPECT images were aligned on a voxel-by-voxel basis using a 3-dimensional automated 6-parameter rigid-body transformation (*10*). ROIs were drawn on the first frame of the bolus study and applied to all other frames, including the frames of the bolus/infusion study, thus generating time–activity curves for striatum and occipital cortex. ROIs were defined according to a standard anatomic atlas. To maximize the statistical quality of the SPECT data, we did not divide the striatum into smaller anatomic regions. The use of whole-striatum ROIs is not applicable in the study of Parkinson's disease and related

disorders because of the possibility of left/right and caudate/putamen asymmetry. In pathologic conditions, coregistration with MR images is beneficial for ROI delineation.

Derivation of Outcome Parameters

Derivation of outcome parameters was based on the 2-tissue-compartment model, which includes the metabolite-corrected plasma compartment (C_1, Bq/mL), the intracerebral nonspecifically bound compartment (C_2, Bq/mL), and the intracerebral specifically bound compartment (C_3, Bq/mL). K_1 (mL/mL/min) and k_2 (/min) denote the rate constants for transfer between C_1 and C_2; k_3 (/min) and k_4 (/min) denote the rate constants for transfer between C_2 and C_3; f_1 (unitless) is the fraction of C_1 free to transfer between C_1 and C_2; and f_2 (unitless) is the fraction of C_2 free to transfer between C_2 and C_1 or C_2 and C_3. Because of the overall physicochemical constancy of brain tissue, the concentration of tracer in C_2 is often assumed to equal the concentration of tracer in an ROI devoid of receptors (C_{ref}).

We defined 2 outcome parameters, BP_1 and BP_2. The transfer of tracer between compartments can be described by a set of 1-order differential equations. A similar set of equations can be written for the simple bimolecular association of a ligand with its receptor. Combining these sets of equations defines BP_1 (unitless) and BP_2 (unitless) in terms of steady-state concentrations of tracer in compartments, rate constants, and binding parameters:

$$BP_1 = \frac{C_3(\infty)}{C_1(\infty)} = \frac{K_1}{k_2}\frac{k_3}{k_4} = BP\ f_1, \qquad \text{Eq. 1}$$

$$BP_2 = \frac{C_3(\infty)}{C_2(\infty)} = \frac{k_3}{k_4} = BP\ f_2. \qquad \text{Eq. 2}$$

$C_1(\infty)$, $C_2(\infty)$, and $C_3(\infty)$ denote the steady-state radiotracer concentration in compartments. SPECT measures the total concentration of radiotracer in the brain (C_{tot}). Because of the overall physicochemical constancy of brain tissue, $C_2(\infty)$ is assumed to equal the concentration of tracer in an ROI devoid of receptors ($C_{ref}(\infty)$), and $C_3(\infty)$ is calculated as $C_{tot}(\infty) - C_{ref}(\infty)$.

The terms BP_1 and BP_2 are the BP of Mintun et al. (1984) (*11*) containing f_1 and f_2, respectively. Those authors used the non–protein-bound fraction of C_1 as a representation of f_1 and calculated f_2 from cerebellar data (assuming $C_{ref} = C_2$) and the measured value of f_1. BP is equal to the ratio of B'_{max} to K_d. B'_{max} (mmol/L) is the concentration of sites available for binding, and K_d (mmol/L) is the affinity constant of the tracer.

Bolus data were analyzed using graphical analysis (*12,13*), kinetic analysis (*14*) with the simplified reference tissue model (*15,16*), peak equilibrium analysis (*17*), and transient equilibrium analysis (*18*). Graphical analysis and kinetic analysis were performed using PMOD version 2.5 (PMOD Technologies). Striatal Logan plots were linear starting at 44 min (range, 30–60 min), and striatal Logan plots using occipital cortex as a representation of the input function were linear starting at 42 min (range, 40–50 min). The 2-tissue-compartment model (mean Akaike information criterion = 57 [range, 46–70]) gave better fits than did the 1-tissue-compartment model (mean Akaike information criterion = 86 [range, 77–96]). The full reference tissue model (*16*) and the simplified reference tissue model (*15*) provided practically identical Akaike information criterion values ($P > 0.12$, paired Student t test) and BP_2 values ($P > 0.26$, paired Student t test). Peak equilibrium analysis was done from 40 to 80 min. This period was based on the range of individual peak times for striatum-specific binding. For calculation of BP_1, the average ^{123}I-PE2I plasma concentration from 40 to 80 min was used. The transient equilibrium analysis was done from 90 to 180 min. The terminal elimination rate constant (a_3) associated with the slowest component of the bolus arterial input curve was determined for each subject. Linear regression analyses were done on logarithmic metabolite-corrected arterial input data from 105 to 175 min. Individual bolus-to-infusion ratios were calculated as $-1/a_3$ (in hours) as previously described (*19*).

RESULTS

Bolus Studies

Figure 2A shows the average time–activity curve for parent compound in arterial plasma. The individual bolus-to-infusion ratios ranged from 1.8 to 3.7 h (Table 1). The 95% confidence intervals for the individual a_3 values were large, and in subject 4 the SE of a_3 was comparable in size to a_3. The 95% confidence intervals of the individual bolus-to-infusion ratios (Table 1) were calculated from the 95% confidence intervals of a_3. An average bolus-to-infusion ratio of 2.5 h was calculated from average a_3 values. This bolus-to-infusion ratio is ideal for attaining a sustained steady state in plasma. We chose to increase the bolus-to-infusion ratio slightly—to 2.7 h—for faster steady-state attainment in the DAT-rich striatal ROI.

Figure 2B shows the average time–activity curves from striatum and occipital cortex. Striatal time–activity curves peaked between 15 and 21 min, and occipital cortex time–activity curves peaked between 3 and 9 min. Striatum-specific binding (striatum – occipital cortex) peaked between 45 and 75 min.

Figures 2C and 2D show the average ratio of striatum-specific binding to metabolite-corrected plasma and the average ratio of striatum-specific binding to occipital cortex, respectively, as a function of time. Starting approximately 90 min after bolus injection, the curves became horizontal.

Figure 3 shows the mean normalized BP_1 and BP_2 values as a function of time after bolus injection of tracer. For each subject, $BP_1(t)$ and $BP_2(t)$ were calculated by deleting a progressive number of frames from the end of the study. For each subject, $BP_1(t)$ and $BP_2(t)$ were normalized to the individual outcome measure calculated at 180 min (using the maximal number of data points). Except for the BP_1 value at 90 min, normalized BPs using kinetic analysis were greater than 90% of the final values from 65 min after ^{123}I-PE2I bolus injection. With the kinetic analysis, the SDs of normalized BP_1 were, however, larger than those obtained with the Logan analysis. The SDs of normalized BP_2, conversely, were comparable to those obtained with the Logan analysis except for the value at 65 min. In contrast to kinetic analysis, with Logan analysis the SDs of the average normalized BPs were less than 10% of the average normalized BP. However, for the Logan approach to be accurate, the acquisition time must be extended beyond 90 min for normalized BPs to be larger than 90% of the final values.

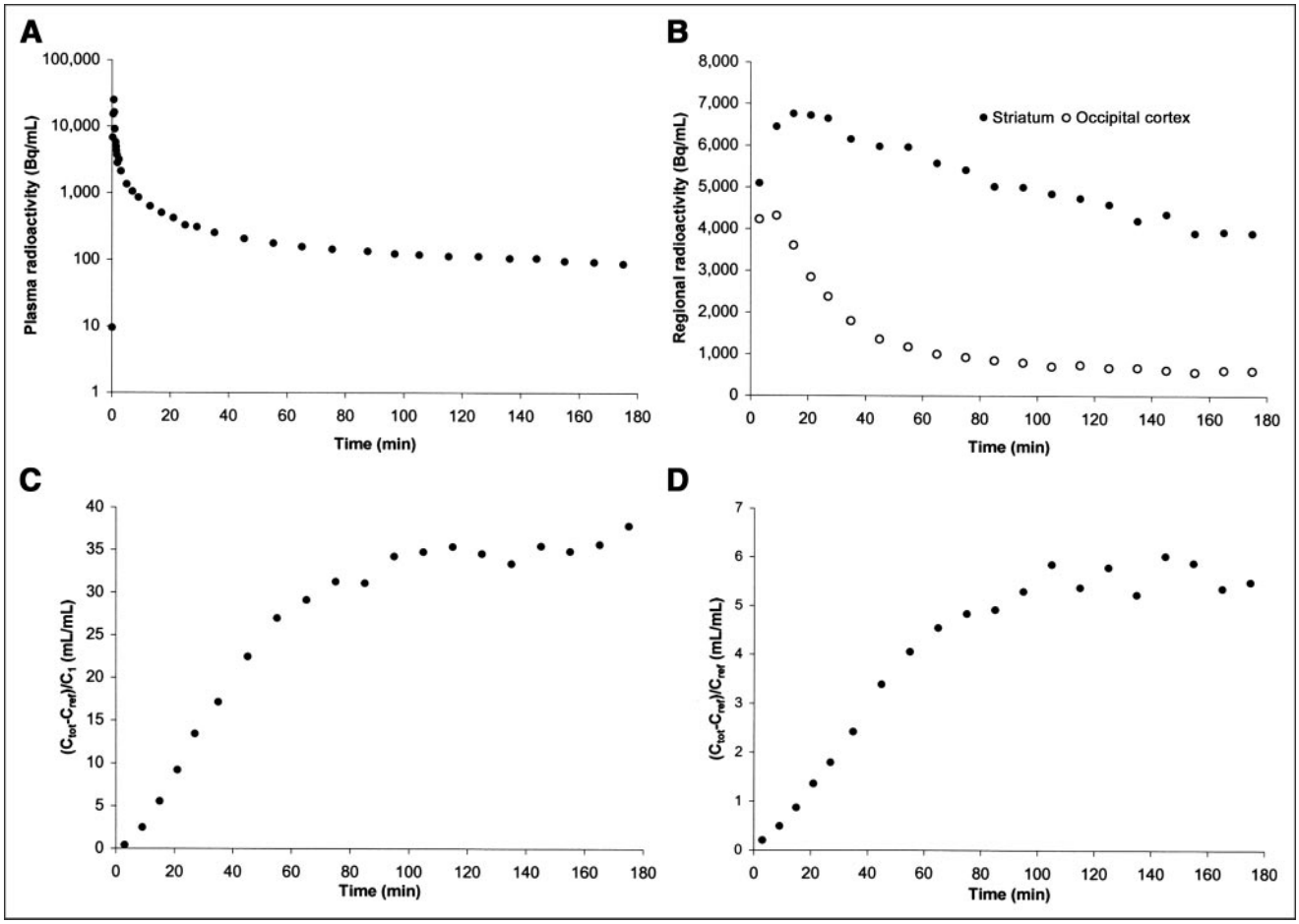

FIGURE 2. Average ^{123}I-PE2I bolus data: time course for metabolite-corrected plasma radioactivity (A), time course for striatum and occipital cortex radioactivity (B), time course for $(C_{tot} - C_{ref})/C_1$ (C), and time course for $(C_{tot} - C_{ref})/C_{ref}$ (D).

The individual and average outcome parameters are listed in Tables 2 and 3. Average striatal BP_1 and BP_2 values as calculated with kinetic analysis were 21.1 ± 1.1 and 4.1 ± 0.4, respectively. Compared with kinetic analyses, Logan analysis underestimated BP_1 by 11% ± 5% ($P < 0.02$, paired Student *t* test) and BP_2 by 3% ± 4% ($P < 0.18$, paired Student *t* test). Compared with kinetic analyses, transient equilibrium analyses overestimated BP_1 by 170% ± 20% ($P < 0.002$, paired Student *t* test) and BP_2 by 136% ± 8% ($P < 0.0002$, paired Student *t* test). Compared with kinetic analyses, peak equilibrium analyses overestimated BP_1 by 133% ± 21% ($P < 0.025$, paired Student *t* test) and BP_2 by 102% ± 7% ($P < 0.5$, paired Student *t* test). The distribution volume equaled the steady-state ratio of tissue

TABLE 1
Stability of Outcome Measures, Free Parent Compound, and Individual Optimal Bolus-to-Infusion Ratio

	Bolus/infusion experiments			Bolus experiments	
Subject no.	BP_1 (%/h)	BP_2 (%/h)	Plasma (%/h)	B/I ratio (h)	Confidence interval (h)
1	−0.1	−4.0	4.2	3.7	2.4–8.5
2	6.8*	2.2	−7.2*	2.4	1.3–12.8
3	−3.1	−6.6	−2.8	3.1	2.8–3.6
4	2.8	2.1	−3.4	2.6	1.3–214.0
5	−6.6	−3.1	−4.2	1.8	1.2–4.0
Average ± SD	−0.0 ± 5.2	−1.9 ± 3.9	−1.6 ± 4.9	2.7 ± 0.7	

*Slope of regression line calculated from 120 to 240 min is significantly different from zero ($P < 0.05$). BP_1, BP_2, and plasma stability measures were calculated from bolus/infusion data. Individual bolus-to-infusion ratios and corresponding 95% confidence intervals were calculated from terminal clearance rate from plasma after bolus injection of ^{123}I-PE2I.

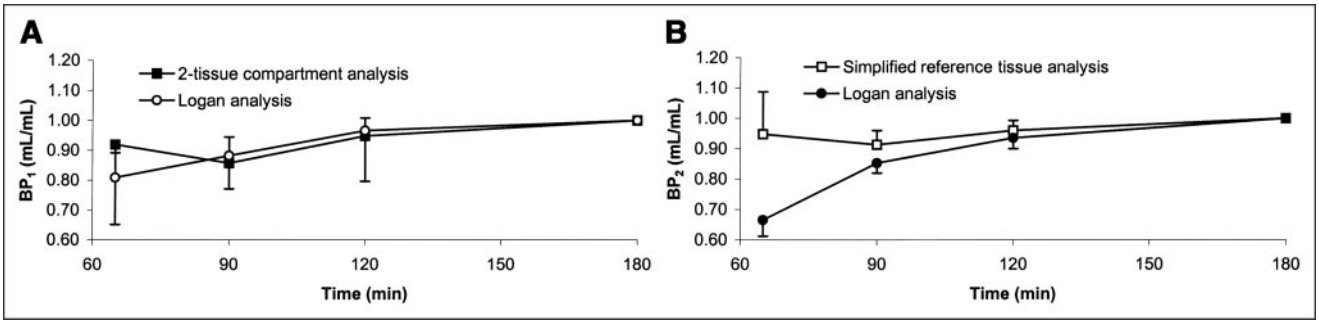

FIGURE 3. (A) Average (with SD) normalized $BP_1(t)$ in striatum calculated using 2-tissue-compartment analysis and Logan analysis with metabolite-corrected plasma as input function. (B) Average (with SD) normalized $BP_2(t)$ in striatum calculated using simplified reference tissue analysis and Logan analysis with occipital cortex as input function. Normalization was performed by dividing value at each time point by value at 180 min. For each method of analysis, average BP_1 and BP_2 were calculated by deleting a progressive number of frames from end of study.

to plasma parent activity and was calculated as $K_1/k_2(1 + k_3/k_4)$ using kinetic analysis. The average striatal distribution volume was 25.9 ± 1.4 mL/mL, and the average occipital cortex distribution volume was 5.0 ± 0.5 mL/mL. In subjects 1–5, the transfer rates from the tissue compartment to plasma (/min) were 0.016 ± 0.001, 0.009 ± 0.001, 0.014 ± 0.001, 0.009 ± 0.001, and 0.011 ± 0.001.

Bolus/Infusion Studies

In Figure 4, each data point represents the mean value of the 5 subjects studied with the average bolus-to-infusion ratio of 2.7 h (Table 1). The average time–activity curves (Figs. 4A and 4B) and outcome measures (Figs. 4C and 4D) plateaued approximately 100–120 min after tracer injection. The stability of the individual time–activity curves and outcome measures was calculated as the slope (linear regression analysis from 120 to 240 min) divided by the average value from 120 to 240 min multiplied by 100%. According to Table 1, individual BP_1, BP_2, and metabolite-corrected plasma radioactivity were stable from 120 to 240 min, with an hourly change of no more than 10%. Except for subject 2, the slopes of the plasma, BP_1, and BP_2 regression lines from 120 to 240 min were not significantly different from zero, but even in this subject, BP_1 and BP_2 were similar to values calculated using kinetic analysis. The individual and average outcome parameters are listed in Tables 2 and 3. Average striatal BP_1 and BP_2 values as calculated with bolus/infusion analysis were 21.0 ± 1.2 and 4.3 ± 0.3, respectively. There was no significant difference between BP_1 calculated using 2-tissue-compartment analysis compared with bolus/infusion analysis (paired Student *t* test, $P > 0.8$, Table 2) and BP_2 calculated using simplified reference tissue analysis compared with bolus/infusion analysis (paired Student *t* test, $P > 0.3$, Table 3). For bolus/infusion analysis, we tested time points ranging from 120 to 180 min and from 180 to 240 min. The average striatal distribution volume was 25.9 ± 1.3 mL/mL, and the average occipital cortex distribution volume was 4.9 ± 0.3 mL/mL.

DISCUSSION

So far, ^{123}I-PE2I has proven to be the ligand with the most favorable in vitro (*1*) and in vivo (*2*) characteristics for DAT quantification in humans using SPECT. The aim of the present study was to describe a method combining accurate, precise quantification of ^{123}I-PE2I binding to DAT and easy implementation in a clinical setting. By conducting the bolus and the bolus/infusion studies on the same subjects, we could eliminate the variation in DAT density that is due to genetic and environmental differences between subjects.

TABLE 2
BP_1 Values Calculated Using 5 Different Methods of Quantification

Subject no.	Bolus/infusion experiments (120–180 min)	Bolus experiments			
		Kinetic analysis (0–180 min)	Logan analysis (0–180 min)	Peak equilibrium (40–80 min)	Transient equilibrium (90–180 min)
1	22.9	21.8	20.4	26.4	31.5
2	20.7	19.8	18.3	31.7	34.0
3	20.6	20.9	19.2	26.0	34.0
4	21.3	20.7	18.1	30.9	41.1
5	19.6	22.6	18.2	24.4	39.0
Average ± SD	21.0 ± 1.2	21.1 ± 1.1	18.8 ± 1.0	27.9 ± 3.2	35.9 ± 4.0

BP_1 was calculated using Equation 1. Peak equilibrium and transient equilibrium were not calculated at tracer steady state.

TABLE 3
BP_2 Values Calculated Using 5 Different Methods of Quantification

Subject no.	Bolus/infusion experiments (120–180 min)	Bolus experiments			
		Reference tissue (0–180 min)	Logan analysis (0–180 min)	Peak equilibrium (40–80 min)	Transient equilibrium (90–180 min)
1	4.6	4.6	4.6	4.8	6.0
2	4.6	4.1	3.7	3.8	5.5
3	4.4	4.3	4.2	4.5	5.5
4	4.0	4.2	4.2	4.7	6.0
5	3.9	3.6	3.5	3.5	5.2
Average ± SD	4.3 ± 0.3	4.1 ± 0.4	4.0 ± 0.4	4.3 ± 0.6	5.6 ± 0.4

BP_2 was calculated using Equation 2. Peak equilibrium and transient equilibrium were not calculated at tracer steady state.

Transient Equilibrium Analysis and Peak Equilibrium Analysis

We found that striatum and occipital cortex time–activity curves peaked within 30 min and that the ratio of striatum-specific binding to nonspecific binding stabilized at an average value of 5.6 ± 0.5 approximately 90 min after ^{123}I-PE2I bolus injection. For comparison, the ratio of striatum-specific binding to nonspecific binding of ^{123}I-FP-CIT, an *N*-fluoropropyl analogue of β-CIT, stabilizes at a value of 2.5 ± 0.6 after approximately 180 min (*20,21*). However, our findings suggest that if transient equilibrium analysis is to be used to calculate DAT density after bolus injection of tracer, ^{123}I-PE2I is preferable to ^{123}I-FP-CIT in terms of both total study time and

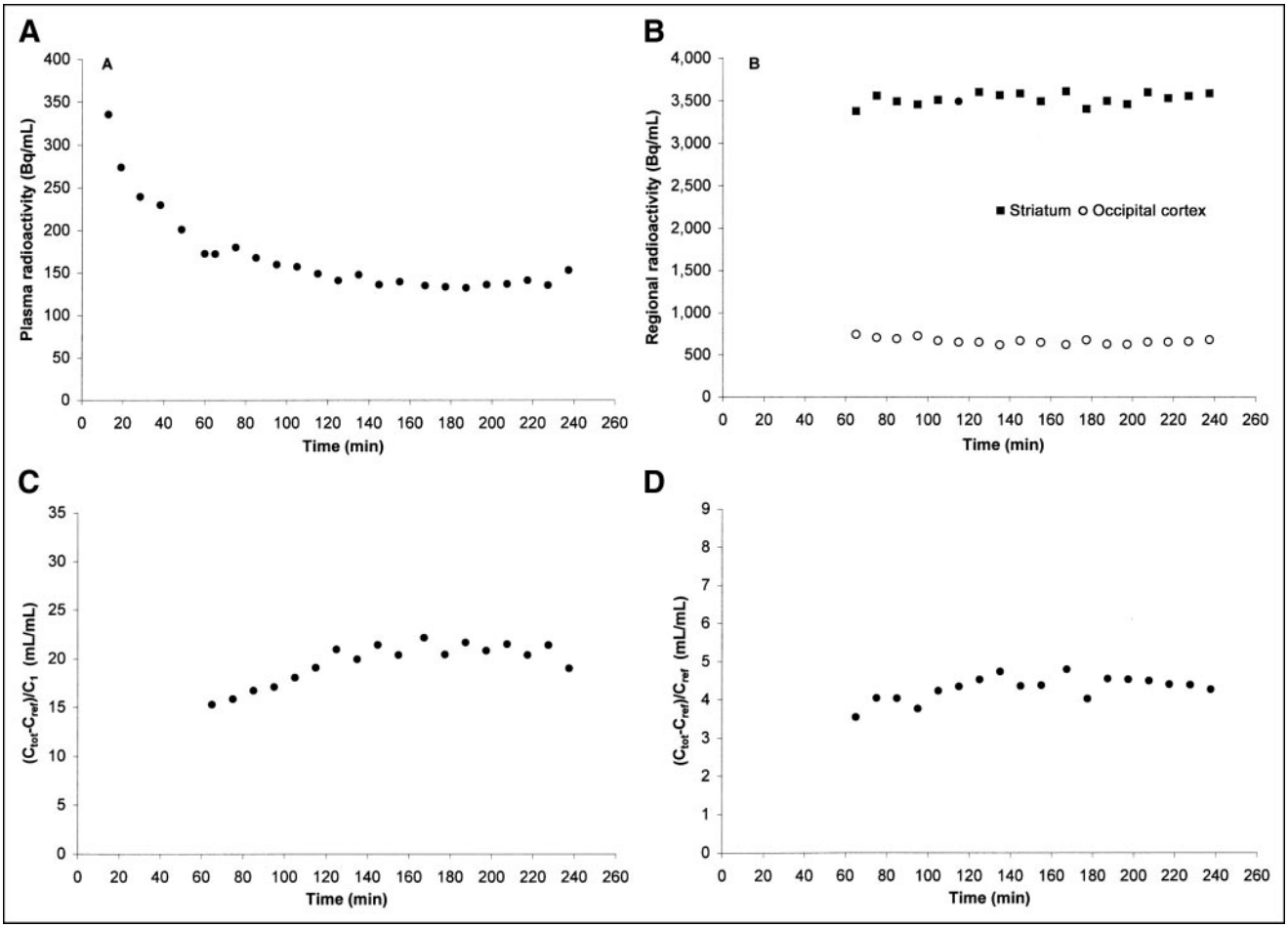

FIGURE 4. Average ^{123}I-PE2I bolus/infusion data: time course for metabolite-corrected plasma radioactivity (A), time course for striatum and occipital cortex radioactivity (B), time course for $(C_{tot} - C_{ref})/C_1$ (C), and time course for $(C_{tot} - C_{ref})/C_{ref}$ (D).

target-to-background ratio. In addition, PE2I has the advantage of being selective for DAT.

In a clinical context, transient equilibrium analysis is easy with respect to tracer administration, data acquisition, and data analysis. However, in addition to transporter/receptor BP, simple tissue-to-blood ratios and tissue-to-tissue ratios calculated at transient equilibrium will reflect the terminal clearance rate from plasma (*18*). According to Table 1, the interindividual variability in the bolus-to-infusion ratios is not negligible (2.7 ± 0.7 h). Furthermore, the terminal clearance rate of ^{123}I-PE2I from plasma is comparable to the transfer rate from the tissue compartment to plasma. Thus, transient equilibrium analysis of ^{123}I-PE2I bolus data overestimates BP_1 and BP_2 values significantly, and BP_1 SEM is large compared with the outcome of a kinetic analysis. In such cases, distinguishing between a normal and a pathologic DAT BP will be more difficult, thus reducing the usefulness of DAT scanning as a clinical tool.

There is no statistical difference between BP_2 calculated using peak equilibrium analysis (40–80 min) and BP_2 calculated using simplified reference tissue analysis, and the SEMs are also comparable. According to Figures 2C and 2D, outcome parameters using peak equilibrium analysis increase rapidly from 0 to 70–80 min, making identification of the correct acquisition period important. In theory, the correct acquisition time must be identified individually around the individual peak time of striatum-specific binding. In practice, a predefined experimentally determined acquisition period is often used. However, striatum-specific time–activity curves will peak earlier in subjects with low BPs than in subjects with high BPs. Thus, applying to Parkinson's disease patients an acquisition time defined in healthy volunteers is likely to overestimate the true BP. Therefore, dynamic acquisition is a sine qua non of peak equilibrium analysis if one is to obtain reliable and comparable BP estimates.

Kinetic Analysis and Logan Analysis

Kinetic analysis and Logan analysis of bolus data are considered gold standards for quantification of radioligand binding to synaptic molecules. Compared with kinetic modeling, Logan analysis is well known to underestimate BP because of the statistical bias associated with linear transformation of binding data (Tables 1 and 2) (*22*). The use of Logan analysis or kinetic analysis in clinical studies is hampered by the need for long study times and arterial blood sampling in case a suitable reference tissue does not exist. Figure 3 addresses the study time needed for accurate and precise quantification of ^{123}I-PE2I binding to DAT using kinetic analysis and Logan analysis. Kinetic analyses (simplified reference tissue analysis in particular) accurately quantify ^{123}I-PE2I binding to DAT starting approximately 60 min after bolus injection. However, for precise quantification of BP_2 using kinetic analysis, the acquisition time must be extended to 90 min. In contrast, Logan analysis precisely quantifies BP_1 and BP_2 starting approximately 60 min after bolus injection. However, for accurate quantification of ^{123}I-PE2I binding to DAT using Logan analysis, the total acquisition time must be at least 90 min after bolus injection. A 90-min total acquisition time after bolus injection of ^{123}I-PE2I is shorter than previously found (120 min) (*3*)—a fact that probably reflects the improved statistical quality of SPECT data using state-of-the-art hardware.

Bolus/Infusion Analysis

The limitations of the transient and peak equilibrium approaches related to nonsteady-state conditions in brain and plasma are overcome in bolus/infusion studies by administration of the tracer as a bolus followed by a constant infusion. As tracer steady state is attained in brain and plasma, the net flux of tracer between compartments becomes zero and the size of the compartments becomes constant, allowing the outcome parameters to be calculated as simple ratios. Several advantages with the bolus/infusion approach deserve consideration: Quantification of binding parameters is insensitive to changes in cerebral blood flow. For tracers without a suitable reference region, venous blood sampling replaces the more invasive arterial blood sampling. For drugs administered as a bolus plus constant infusion at pharmacologic doses, the acute effect on binding parameters may be calculated within a single scan session after a single radioligand synthesis. If scanning has to be aborted before the scheduled time because of patient discomfort or other causes, quantification of binding parameters may still be possible despite the reduced statistical quality of the data.

The bolus/infusion approach also has some disadvantages: To hasten steady state, a bolus of radiolabeled ligand must be administered, but the optimal bolus-to-infusion ratio required to hasten steady state may vary considerably because of differences in tracer clearance and receptor binding between individuals. In this study, individual bolus-to-infusion ratios ranged from 1.8 to 3.7 h (Table 1), and a bolus-to-infusion ratio of 2.7 h was used in all subsequent bolus/infusion studies. For fast attainment of steady state in plasma, a bolus-to-infusion ratio of 2.5 h ($-1/\text{average}(a_3)$) would have been ideal. To hasten attainment of steady state in striatum, we increased the bolus-to-infusion ratio from 2.5 to 2.7 h. Post hoc computer simulations based on the bolus data suggested that a bolus-to-infusion ratio of 2.9 h would have more rapidly attained stable striatal BP_1 and BP_2 values. However, the average experimental data imply that a bolus-to-infusion ratio of 2.7 h quickly attains stable striatal ^{123}I-PE2I concentrations (Fig. 4B), with a modest overshoot in the plasma (Fig. 4A) and occipital cortex (Fig. 4B) ^{123}I-PE2I concentrations. Further increasing the bolus-to-infusion ratio and, thus, the overshoot in occipital cortex and plasma is likely to slow the attainment of stable values for BP_1 (Fig. 4C) and BP_2 (Fig. 4D). The size and sign of the percentage change in plasma ^{123}I-PE2I concentrations per hour were in agreement with the individual bolus-determined optimal bolus-to-infusion ratios. For BP_1 and BP_2, the percentage change per hour, compared with the individual bolus-determined optimal bolus-to-infusion ratio, was

less consistent with expectations. However, in all subjects, individual BP_1, BP_2, and metabolite-corrected plasma radioactivity were stable (defined as a change of no more than 10%/h) from 120 to 240 min after bolus/infusion of ^{123}I-PE2I, and BP_1 and BP_2 values calculated using bolus/infusion analysis were not significantly different from values calculated using kinetic analysis. This finding is remarkable considering the range of individual bolus-to-infusion ratios. However, as discussed in the Appendix, computer simulations demonstrate that a 2-fold variation in terminal clearance rate from plasma translates into only a 10% variation in the BPs calculated from 120 to 180 min. Furthermore, estimated a_3 values are calculated from the noisy terminal part of the metabolite-corrected plasma time–activity curve, and the 95% confidence intervals are large. Thus, the individual "true" a_3 values may be more similar than is indicated by the estimated a_3 values. Comparing the individual size of BP_1 calculated using transient equilibrium analysis ($K_1/(k_2 + a_3)$) (*18*) with the individual size of BP_1 calculated using kinetic analysis (K_1/k_2) supports this idea.

CONCLUSION

Graphical analysis and kinetic analysis quantify ^{123}I-PE2I-bolus data both accurately and precisely. However, in a clinical setting, a total scan time of 90 min may be too inconvenient. With respect to experimental simplicity, transient equilibrium analysis is an attractive and widely used method in nuclear medicine. However, for PE2I and many other ligands with terminal clearance rates from plasma comparable to the transfer rates from the tissue compartment, clinical feasibility is hampered by low accuracy and significantly reduced precision. According to our data from healthy volunteers, peak equilibrium analysis allows accurate, precise calculation of BP_2. However, accuracy and precision depend on precise identification of the peak time of specific binding, because the apparent BP_2 value doubles from 40 to 80 min. Thus, in patients with changes in DAT density, total time spent in the scanner must be increased to identify individual peak times. The bolus/infusion approach quantifies ^{123}I-PE2I bolus/infusion data both accurately and precisely. According to experimental data and computer simulations, individual differences in terminal clearance rates from plasma do not affect outcome parameters after 120 min of constant ^{123}I-PE2I infusion. Some may consider the need for a constant infusion of tracer to be an important limitation for clinical studies. In our experience, the increase in experimental complexity is small compared with the advantages of the bolus/infusion approach. We have implemented the bolus/infusion approach for clinical studies of DAT using ^{123}I-PE2I SPECT.

APPENDIX

It is possible to simulate the outcome of a bolus/infusion study using the kinetic parameters calculated from a bolus-

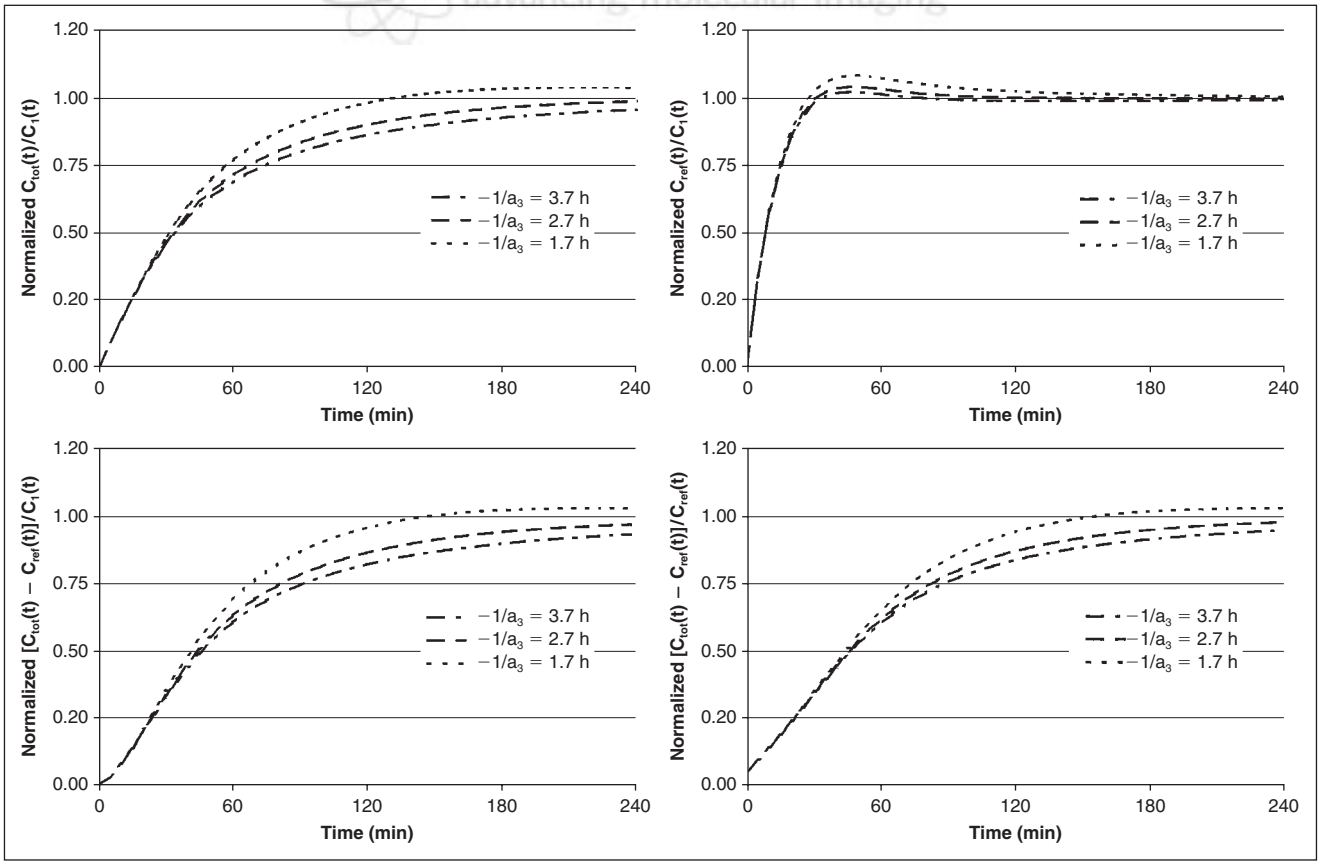

FIGURE 1A. Computer simulations of outcome parameters after bolus plus constant infusion of radiotracer. See text for details.

alone study (*23*). The bolus input function is approximated to a sum of 3 exponential functions ($\sum_{i=1}^{3} A_i e^{a_i t}$), and in the 1-tissue-compartment situation, K_1 and k_2 values are calculated using kinetic analysis:

$$C_1(t) = \sum_{i=1}^{3} A_1\left(\left(B/I - \frac{1}{-a_i}\right)e^{a_i t} + \frac{1}{-a_i}\right), \qquad \text{Eq. 1A}$$

$$C_{tot}(t) = \sum_{i=1}^{3} A_i\left(\left(B/I - \frac{1}{-a_i}\right)\frac{K_1}{k_2 + a_i}(e^{a_i t} - e^{-k_2 t}) + \frac{1}{-a_i}\frac{K_1}{k_2}(1 - e^{-k_2 t})\right), \qquad \text{Eq. 2A}$$

$$C_{ref}(t) = \sum_{i=1}^{3} A_i\left(\left(B/I - \frac{1}{-a_i}\right)\frac{K_1^{ref}}{k_2^{ref} + a_i}(e^{a_i t} - e^{-k_2^{ref} t}) + \frac{1}{-a_i}\frac{K_1^{ref}}{k_2^{ref}}(1 - e^{-k_2^{ref} t})\right), \qquad \text{Eq. 3A}$$

where B/I (h) is the bolus-to-infusion ratio, A_i (unitless) is the relative zero intercept of each exponential, and a_i (/min) is the elimination rate constant associated with each exponential. Figure 1A shows simulated outcome parameters from 0 to 240 min. Outcome parameters are calculated using Equations 1A–3A. Total distribution volume = $C_{tot}(t)/C_1(t)$, reference distribution volume = $C_{ref}(t)/C_1(t)$, $BP_1(t) = (C_{tot}(t) - C_{ref}(t))/C_1(t)$, and $BP_2(t) = (C_{tot}(t) - C_{ref}(t))/C_{ref}(t)$. Values have been normalized with the individual steady-state values. In all situations, B/I = 2.7 h, $a_1 = -0.6$/min, $a_2 = -0.06$/min, $K_1 = 0.42$ mL/mL/min, $k_2 = 0.016$/min, $K_1^{ref} = 0.35$ mL/mL/min, and $k_2^{ref} = 0.068$/min. Individual curves represent situations with different terminal clearance rates from plasma (a_3). In the keys, the individual a_3 value is expressed as $-1/a_3$ (h), representing the individual optimal bolus-to-infusion ratio. The simulations demonstrate 2 important points on the use of the bolus/infusion approach. First, calculations of BP_1 and BP_2 using a population-based average bolus-to-infusion ratio are clearly vulnerable to individual differences in terminal clearance rate from plasma. However, the vulnerability decreases with time. From 120 to 180 min, the average normalized BP_1 values are 1.01 ($-1/a_3 = 1.7$ h), 0.92 ($-1/a_3 = 2.7$ h), and 0.87 ($-1/a_3 = 3.7$ h) and the average normalized BP_2 values are 0.99 ($-1/a_3 = 1.7$ h), 0.92 ($-1/a_3 = 2.7$ h), and 0.88 ($-1/a_3 = 3.7$ h). Thus, a 2.2-fold variation in terminal clearance rate from plasma translates into only a 10% variation in the calculated BPs. Second, to hasten attainment of steady-state BPs, it is beneficial to increase the bolus-to-infusion ratio beyond the value calculated from the average a_3 value.

ACKNOWLEDGMENTS

We thank Gerda Thomsen, Karin Stahr, Inge Møller, and Anja Pedersen for expert technical assistance. This work was supported by the Danish Health Research Council, the 1991 Pharmacy Foundation Health Insurance Fund, the Lundbeck Foundation, the Elsass Foundation, and the University of Copenhagen.

REFERENCES

1. Emond P, Garreau L, Chalon S, et al. Synthesis and ligand binding of nortropane derivatives: N-substituted 2beta-carbomethoxy-3beta-(4′-iodophenyl)nortropane and N-(3-iodoprop-(2E)-enyl)-2beta-carbomethoxy-3beta-(3′,4′-disubstituted phenyl)nortropane—new high-affinity and selective compounds for the dopamine transporter. *J Med Chem.* 1997;40:1366–1372.
2. Halldin C, Erixon-Lindroth N, Pauli S, et al. [(11)C]PE2I: a highly selective radioligand for PET examination of the dopamine transporter in monkey and human brain. *Eur J Nucl Med Mol Imaging.* 2003;30:1220–1230.
3. Kuikka JT, Baulieu JL, Hiltunen J, et al. Pharmacokinetics and dosimetry of iodine-123 labelled PE2I in humans, a radioligand for dopamine transporter imaging. *Eur J Nucl Med.* 1998;25:531–534.
4. Pinborg LH, Videbaek C, Svarer C, Yndgaard S, Paulson OB, Knudsen GM. Quantification of [(123)I]PE2I binding to dopamine transporters with SPET. *Eur J Nucl Med Mol Imaging.* 2002;29:623–631.
5. Prunier C, Payoux P, Guilloteau D, et al. Quantification of dopamine transporter by ^{123}I-PE2I SPECT and the noninvasive Logan graphical method in Parkinson's disease. *J Nucl Med.* 2003;44:663–670.
6. Hall H, Halldin C, Guilloteau D, et al. Visualization of the dopamine transporter in the human brain postmortem with the new selective ligand [^{125}I]PE2I. *Neuroimage.* 1999;9:108–116.
7. Videbaek C, Knudsen GM, Bergstrom K, et al. Octanol extraction yields similar results as HPLC for quantitation of [^{123}I]PE2I metabolism [abstract]. *Eur J Nucl Med.* 1999;26:1139.
8. Poyot T, Conde F, Gregoire MC, et al. Anatomic and biochemical correlates of the dopamine transporter ligand ^{11}C-PE2I in normal and parkinsonian primates: comparison with 6-[^{18}F]fluoro-L-dopa. *J Cereb Blood Flow Metab.* 2001;21:782–792.
9. Prunier C, Bezard E, Montharu J, et al. Presymptomatic diagnosis of experimental Parkinsonism with ^{123}I-PE2I SPECT. *Neuroimage.* 2003;19:810–816.
10. Woods RP, Cherry SR, Mazziotta JC. Rapid automated algorithm for aligning and reslicing PET images. *J Comput Assist Tomogr.* 1992;16:620–633.
11. Mintun MA, Raichle ME, Kilbourn MR, Wooten GF, Welch MJ. A quantitative model for the in vivo assessment of drug binding sites with positron emission tomography. *Ann Neurol.* 1984;15:217–227.
12. Logan J, Fowler JS, Volkow ND, et al. Graphical analysis of reversible radioligand binding from time-activity measurements applied to [N-^{11}C-methyl]-(−)-cocaine PET studies in human subjects. *J Cereb Blood Flow Metab.* 1990;10:740–747.
13. Logan J, Fowler JS, Volkow ND, Wang GJ, Ding YS, Alexoff DL. Distribution volume ratios without blood sampling from graphical analysis of PET data. *J Cereb Blood Flow Metab.* 1996;16:834–840.
14. Koeppe RA, Holthoff VA, Frey KA, Kilbourn MR, Kuhl DE. Compartmental analysis of [^{11}C]flumazenil kinetics for the estimation of ligand transport rate and receptor distribution using positron emission tomography. *J Cereb Blood Flow Metab.* 1991;11:735–744.
15. Lammertsma AA, Hume SP. Simplified reference tissue model for PET receptor studies. *Neuroimage.* 1996;4:153–158.
16. Hume SP, Myers R, Bloomfield PM, et al. Quantitation of carbon-11-labeled raclopride in rat striatum using positron emission tomography. *Synapse.* 1992;12:47–54.
17. Farde L, Eriksson L, Blomquist G, Halldin C. Kinetic analysis of central [^{11}C]raclopride binding to D_2-dopamine receptors studied by PET: a comparison to the equilibrium analysis. *J Cereb Blood Flow Metab.* 1989;9:696–708.
18. Carson RE, Channing MA, Blasberg RG, et al. Comparison of bolus and infusion methods for receptor quantitation: application to [^{18}F]cyclofoxy and positron emission tomography. *J Cereb Blood Flow Metab.* 1993;13:24–42.
19. Pinborg LH, Adams KH, Svarer C, et al. Quantification of 5-HT2A receptors in the human brain using [^{18}F]altanserin-PET and the bolus/infusion approach. *J Cereb Blood Flow Metab.* 2003;23:985–996.
20. Booij J, Bergmans P, Winogrodzka A, Speelman JD, Wolters EC. Imaging of dopamine transporters with [^{123}I]FP-CIT SPECT does not suggest a significant effect of age on the symptomatic threshold of disease in Parkinson's disease. *Synapse.* 2001;39:101–108.
21. Booij J, Hemelaar TG, Speelman JD, de Bruin K, Janssen AG, van Royen EA. One-day protocol for imaging of the nigrostriatal dopaminergic pathway in Parkinson's disease by [^{123}I]FPCIT SPECT. *J Nucl Med.* 1999;40:753–761.
22. Slifstein M, Laruelle M. Effects of statistical noise on graphic analysis of PET neuroreceptor studies. *J Nucl Med.* 2000;41:2083–2088.
23. Pinborg LH, Videbaek C, Knudsen GM, et al. Dopamine D(2) receptor quantification in extrastriatal brain regions using [(123)I]epidepride with bolus/infusion. *Synapse.* 2000;36:322–329.